Chapter 5
A First Experience with Multidimensional Contact Real-Time Hybrid Substructuring: Toward Testing of Foot Prostheses

Arian Kist, Talhah Ansari, Christina Insam, and Daniel Rixen

Abstract Real-time hybrid substructuring (RTHS) is a promising approach to investigate the influence of foot prostheses on the gait pattern in versatile situations, while avoiding the necessity to model the prosthesis and its ground interaction. A numerical gait simulation is coupled in real-time to a prosthesis prototype on a test rig using sensors and actuators. However, synchronization errors make such experiments prone to instabilities. Thus, methods are required to ensure robust and stable RTHS experiments. In previous work, we developed promising methods using a one-dimensional contact RTHS experiment. In this contribution, we show our first experience with multidimensional contact RTHS in order to take the next step to enable foot prosthesis RTHS experiments. We present the design of a simplified planar foot prosthesis RTHS setup. Furthermore, we show the first results of a virtual RTHS test, where test stability is ensured through the application of normalized passivity control (NPC). From these results, we conclude that our approach is promising to extend our previously developed methods to the multidimensional case.

Keywords Real-time hybrid substructuring · Prosthesis testing · Passivity control · Hardware-in-the-loop · Hybrid simulation

5.1 Introduction

The development of prostheses for the lower human limb, which accurately reproduce the gait of able-bodied humans, has high relevance in the modern aging society. Especially, widespread diseases like diabetes mellitus and peripheral arterial disease are some of the major causes of a lower limb amputation. Even though the total number of lower limb amputations has been decreasing in recent years, still more than 60,000 lower limb amputations were registered in Germany in 2019 [1]. After such an amputation, the amputees rely on using a prosthesis in order to restore their ability to walk. Prosthetics have been used for centuries to support amputees, and, in general, prosthetics are a great help to let amputees walk again. Nonetheless, they still have major shortcomings due to the complexity of the biological counterpart. The gait of an amputee wearing the prosthesis is altered compared to the gait of an able-bodied person. A long-term imbalanced loading of the legs during walking can lead to bone and joint diseases. [2, 3] To overcome these problems, the influence of the prosthesis on the gait of the amputee must be considered from an early development stage on. Nevertheless, the investigation of lower limb prostheses together with a walking amputee is cumbersome. A pure stimulative approach is often not feasible since it requires the development and validation of an accurate numerical model of the prosthesis, which is an ambitious and time-consuming process. Another approach would consist of testing the prosthesis with human test subjects. Although this avoids the modeling and gives great insight into how the gait is altered, the test results are subjective to the specific test persons and test scenario. [4, 5] To conclude, methods are required that combine the advantages of prototype-based and simulation-based testing.

Real-time hybrid substructuring (RTHS) is a mechanical hardware-in-the-loop method to investigate complex dynamic structures economically and with high accuracy. This method originates from structural testing in earthquake engineering, but can be used for all kinds of dynamic structures. In RTHS, the dynamic system to investigate is partitioned into a numerical substructure and an experimental substructure. The former is simulated numerically, while for the latter a prototype is built and investigated on a test rig. To replicate the system dynamics of the whole system, the numerical part and the experimental

A. Kist (✉) · T. Ansari · C. Insam · D. Rixen
Chair of Applied Mechanics, School of Engineering and Design, Technical University of Munich, Garching, Germany
e-mail: arian.kist@tum.de; talhah.ansari@tum.de; rixen@tum.de

© The Society for Experimental Mechanics, Inc. 2024

M. Allen et al. (eds.), *Dynamic Substructures, Volume 4*, Conference Proceedings of the Society for Experimental Mechanics Series, https://doi.org/10.1007/978-3-031-36694-9_5

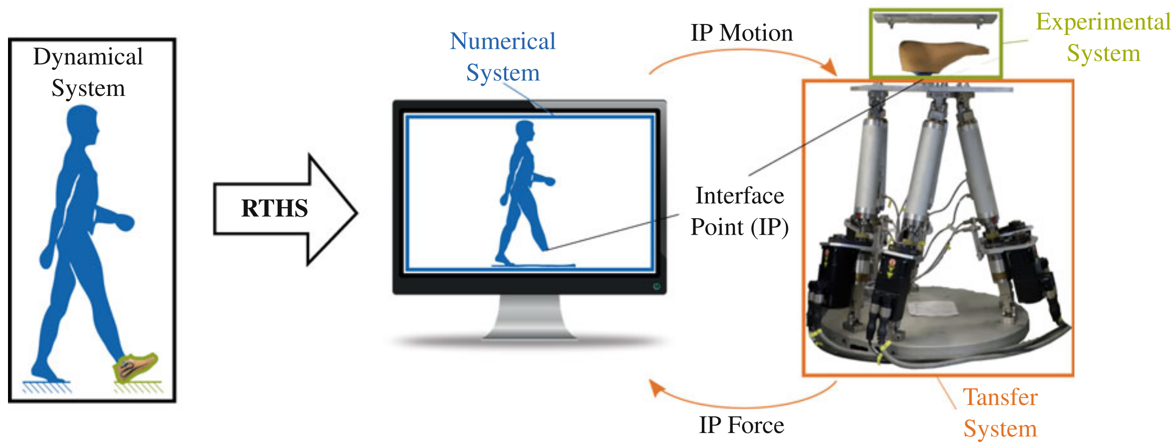

Fig. 5.1 RTHS principle visualized using the example of testing foot prostheses. Herein, the gait of an amputee is simulated numerically and coupled in real-time to a real foot prosthesis on a test rig. Thereby, the dynamic interplay between both subsystems is emulated and the influence of the prosthesis on the amputee's gait can be investigated (Image of the amputee adapted from [11]; figure adapted from [5])

part are coupled in real-time using a transfer system [6–8]. This enables to investigate systems, where some parts or effects cannot be modeled properly. By investigating only these critical parts experimentally on a test rig and coupling their response to the numerical model of the remaining structure in real-time, the systems dynamics of the whole system are preserved. By transferring this method to investigate lower limb prostheses and their influence on the gait of the amputee, the abovementioned drawback of the current test procedures can be overcome. The idea of using RTHS for the assessment of foot prostheses was proposed by *Yang et al.* [9] and further pursued by *Insam et al.* [5, 10]. The concept is visualized in Fig. 5.1. The dynamic system to investigate is a human wearing a foot prosthesis. Since the prosthesis is the critical structure, it is investigated experimentally. The remainder, which is the walking amputee, is simulated numerically. Note that, even though the modeling of the amputee is highly complex, this approach offers the advantage that the dynamic interaction between the amputee and the prosthesis can be investigated without putting a person at risk. Furthermore, several physical quantities, like hip torque, muscle activation, etc., can be measured from the numerical simulation, which would not be easily possible in a human. The motion of the interface point (IP), which is the point where the prosthesis is mounted, is calculated by the numerical system and sent as a command to a controlled actuator. This actuator, which is a Stewart Platform in Fig. 5.1, executes this motion.[1] The forces and torques at the IP resulting from this motion are measured and fed back to the numerical system. Consequently, the next time integration step of the numerical simulation is performed, which results in a new value for the IP motion and is sent as the next command to the actuator. Since the whole RTHS loop runs in real-time, the true dynamic properties of the amputee walking with the prosthesis can be emulated. This enables a highly versatile investigation of the influence of the prosthesis on the human gait in many different scenarios without modeling the prosthesis.

Although this approach is promising, it involves many challenges. Testing foot prosthesis is a multidimensional contact scenario, which means it comes into contact with the ground intermittently. Hence, the system dynamics exhibit discontinuities. As reported in [9, 10], RTHS tests for such systems are prone to instabilities, which cause the test fidelity to decrease heavily and potentially damage the test rig. These instabilities can be traced back to a nonideal transfer system, that is, imperfect actuator tracking, in combination with RTHS tests including contact. Thus, in our previous work [12–15], we intensively investigated control approaches to ensure robust and stable RTHS experiments with contact. Despite showing great potential, the methods were only tested and validated using a one-dimensional RTHS scenario. Since testing of foot prostheses is a multidimensional contact scenario, we aim at the extension and validation of the developed methods using multidimensional contact RTHS scenarios. Note that, in [5], a first preliminary RTHS test using a real foot prosthesis as experimental system was performed. Despite proving the general applicability of RTHS to investigate foot prostheses, the transfer system used here was not powerful and fast enough to test our methods to improve the interface tracking and guarantee stability.

In this contribution, we present our first experience with multidimensional contact RTHS experiments. We design a simplified planar foot prosthesis model to be investigated with RTHS. This model provides the advantage that in contrast to real foot prosthesis the dynamic response of the simplified system can be fully modeled. Thus, we can compare our RTHS

[1] Note that the prosthesis is mounted upside down on the actuator, which must be compensated for.

results to a reference simulation. Furthermore, we show the first results of a virtual RTHS test (that is the transfer system and the experimental system are simulated numerically as well), including the application of normalized passivity control (NPC).

5.2 System Design

In order to take a step further to the testing of foot prostheses with RTHS, a simplified planar foot model shown in Fig. 5.2 was developed. It consists of two rigid bodies with the masses m_{NUM} and m_{EXP}, respectively. The lower body is a thin beam with the length l_{EXP} representing a foot prosthesis. The upper body is a disc with radius r_{NUM} and represents the remaining part of an amputated leg. The upper body is excited in the x- and y-direction via spring-damper couplings ($k_{\mathrm{p,x}}$, $k_{\mathrm{d,x}}$ and $k_{\mathrm{p,y}}$, $k_{\mathrm{d,y}}$) to an exciting motion $x_{\mathrm{ex}}(t)$ and $y_{\mathrm{ex}}(t)$. The disc can rotate with the angle ϕ_{NUM} and a rotation $\phi_{\mathrm{ex}}(t)$ is imposed at the basis of a rotational spring-damper-system ($k_{\mathrm{p},\phi}$, $k_{\mathrm{d},\phi}$). This corresponds to controlling the disk to a desired motion using PD controllers. To connect the disk to the lower body, again spring-damper couplings are used. Both spring-damper-systems rotate with ϕ_{NUM}. One spring-damper-system ($k_{\mathrm{p,par}}$, $k_{\mathrm{d,par}}$) is parallel to the axis connecting the interface points on both masses. This spring has the undeformed length l_0. The other spring-damper-system ($k_{\mathrm{p,per}}$ and $k_{\mathrm{d,per}}$) is perpendicular to this connecting axis and is undeformed if there is no relative perpendicular displacement of the interface points. The beam can rotate with ϕ_{EXP}. Thus, the beam is additionally connected to the disc via a rotational spring-damper-system ($k_{\mathrm{p,rot}}$ and $k_{\mathrm{d,rot}}$). The interface point of the beam is shifted in beam direction with the distance a from the center of mass (CoM). Note that the simplicity of the system allows us to determine a reference simulation for the RTHS experiment, which would be much more challenging for a real foot prosthesis RTHS. Nevertheless, with the described system we can investigate multidimensional contact RTHS similar to a foot prosthesis RTHS. In order to model the ground contact, two distinct contact points (CP_1 and CP_2) at each end of the beam can come into contact with the ground and thus experience a ground reaction force. For the ground contact modeling, we refer to the next section.

The substructuring into the numerical part (blue) and experimental part (green) is indicated in Fig. 5.2. The upper disk, together with the exciting motion, is chosen as a numerical subsystem. The interface couplings, the beam, and the ground contact are consequently the experimental subsystem.

5.3 Simulation Setup

In order to gain a first experience with the designed model and the respective RTHS experiments, we developed a digital twin for the whole RTHS loop. In this purely virtual RTHS, in addition to the numerical subsystem also the transfer system and the experimental system are numerically simulated. The simulation was implemented using *Mathworks* MATLAB/Simulink (Version R2022a). All simulation parameters are given in Table 5.1.

The numerical mass m_{NUM} is excited using an external motion that acts on the disc via spring-damper-systems as seen in Fig. 5.2. We chose the exciting trajectories as follows:

$$x_{\mathrm{ex}}(t) = -A_{\mathrm{x}} \cos\left(2\pi \frac{f_{\mathrm{d}}}{2} t\right) + A_{\mathrm{x}} + x_{\mathrm{NUM},0} \tag{5.1}$$

$$y_{\mathrm{ex}}(t) = \frac{y_{\mathrm{EXP},0} + A_{\mathrm{y}}}{2} \cos\left(2\pi f_{\mathrm{d}} t\right) - \frac{y_{\mathrm{EXP},0} + A_{\mathrm{y}}}{2} + y_{\mathrm{NUM},0} \tag{5.2}$$

$$\phi_{\mathrm{ex}}(t) = A_{\phi} \cos\left(2\pi \frac{f_{\mathrm{d}}}{2} t\right) - A_{\phi} + \phi_{\mathrm{NUM},0} \tag{5.3}$$

Note that quantities with a $\bullet_{\bullet,0}$ as second index denote an initial value. Furthermore, it has to be mentioned that these trajectories are chosen just to ensure a planar RTHS test with ground contact and zero velocities at the beginning and end of the trajectories. We do not aim to reproduce human gait characteristics by this choice. All forces acting on m_{NUM} are due to spring-damper systems, and thus, its equations of motions can be solved in order to simulate the motion of m_{NUM}. The motion of the IP $\mathbf{q}_{\mathrm{IP}}$ is sent as motion command to our controlled actuator (see Fig. 5.2). In our setup, this actuator is an in-house-built Stewart Platform controlled using a decentralized cascaded P-PI-PI joint control with no feedforward controller. In order to simulate the dynamic response of the actuator up to 100 Hz, we use second-order transfer functions,

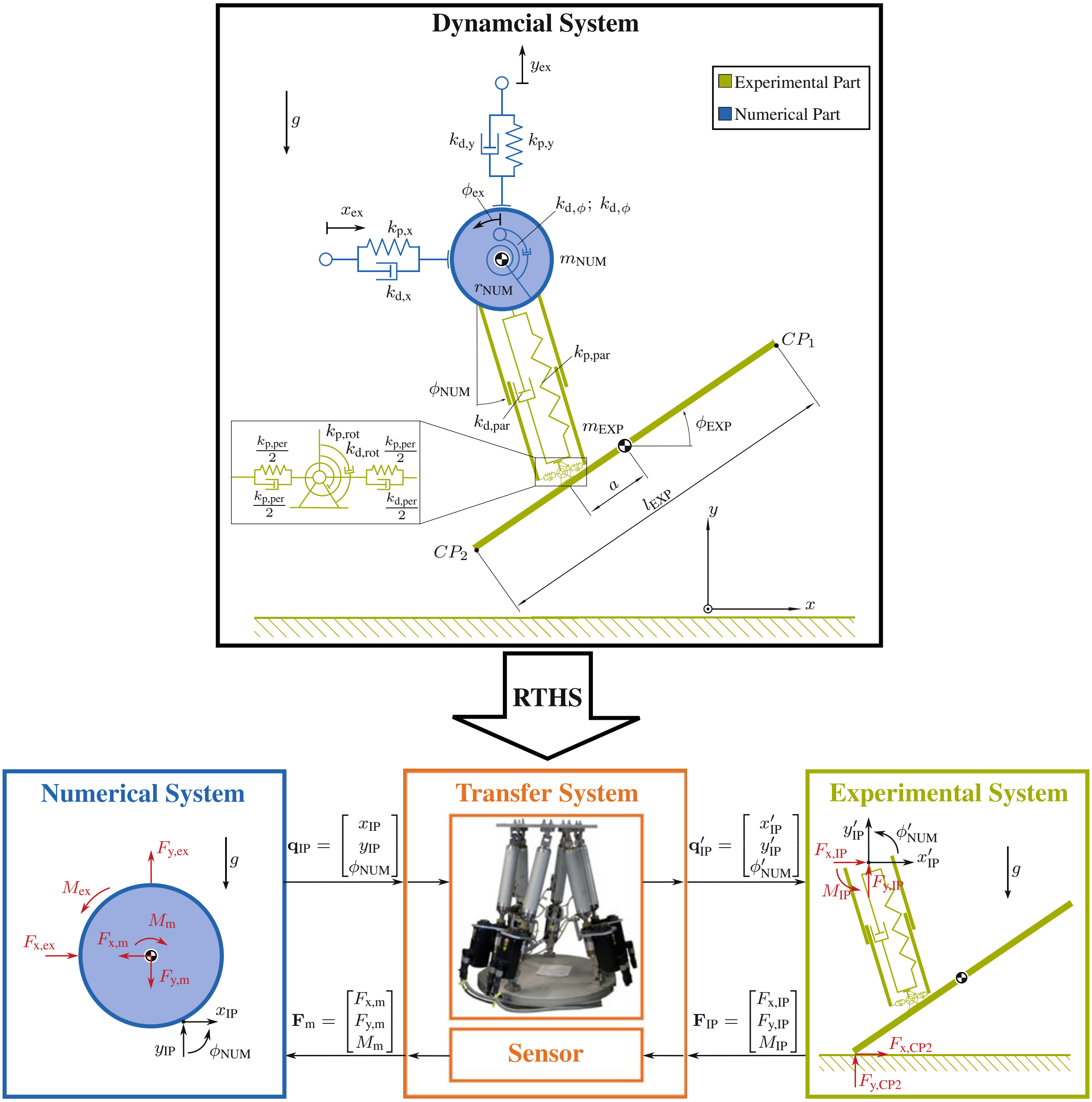

Fig. 5.2 Simplified planar foot prosthesis RTHS scenario. The upper part of this figure shows the dynamic system to be investigated using RTHS in detail. The lower part of this figure shows the RTHS setup with the respective substructures and the interface quantities

determined in previous work. For more information on the controller and the system identification, we refer to our previous publication [15]. Due to a nonideal tracking performance, the actuator executes the motion $\mathbf{q}'_{IP} \neq \mathbf{q}_{IP}$. The force-torque-sensor, measuring the interface force, is assumed to be ideal for our digital twin, thus $\mathbf{F}_m = \mathbf{F}_{IP}$. As mentioned, we also simulate the dynamic behavior of the experimental system in our virtual RTHS. To model the ground contact, the method by *Geyer and Herr* [16] was implemented. This model assumes two distinct contact points (CP_1 and CP_2) at the toe and the heel, where the contact to the ground occurs. The vertical (y-direction) ground reaction force is calculated based on a nonlinear spring-damper model, which is activated during ground penetration. The horizontal (x-direction) ground reaction force models static and kinetic friction. The static friction force is calculated as nonlinear spring-damper-system similar to the vertical ground reaction force. The force during kinetic friction is calculated based on the vertical ground reaction force and

Table 5.1 Parameters used for the simulation. Note that all initial values (denoted by a 0 as second index) are chosen in a way that each spring is initially in its static equilibrium.

Variable	Value	Variable	Value	Variable	Value
A_x	0.015 m	A_y	0.005 m	A_ϕ	$\frac{\pi}{16}$ rad
f_d	0.25 Hz	$k_{p,x} = k_{p,y}$	10^4 N/m	$k_{d,x} = k_{d,y}$	75 Ns/m
$k_{p,\phi}$	100 N/rad	$k_{d,\phi}$	5 Ns/rad	$k_{p,par}$	8650 N/m
$k_{d,par}$	10 Ns/m	$k_{p,per}$	10^6 N/m	$k_{d,per}$	500 Ns/m
$k_{p,rot}$	0.5 N/rad	$k_{d,rot}$	0.01 Ns/rad	l_0	0.071 m
a	0.005 m	r_{NUM}	0.01 m	l_{EXP}	0.03 m
g	9.81 m/s^2	m_{NUM}	9.6187 kg	m_{EXP}	0.3813 kg
$\phi_{NUM,0}$	$\frac{\pi}{8}$ rad	$y_{NUM,0}$	0.0835 m	$x_{NUM,0}$	0 m
$\phi_{EXP,0}$	0.3581 rad	$y_{EXP,0}$	0.01 m	$x_{EXP,0}$	0.358 m
ΔT	10^{-4} s	Solver	ode1 (Euler)	t_{stop}	4 s
G_p	800	T_{LP}	0.05 s	–	–

a sliding friction coefficient. Note that compared to the implementation by *Geyer and Herr*, we increased the vertical ground stiffness by a factor of ten in order to decrease ground penetration (all other parameters for the ground contact modeling were chosen as published in [16]). Based on the actual IP motion $\mathbf{q}'_{IP}$ and the ground contact, all forces acting on m_{EXP} are determined and its dynamic behavior can be simulated.

5.4 Normalized Passivity Control (NPC)

NPC is a control approach to ensure stability of RTHS experiments, countering the abovementioned stability problems. This approach was originally proposed by *Peiris et al.* [17] and applied to one-dimensional RTHS experiments. *Insam et al.* [13, 14] further investigated this approach using one-dimensional RTHS experiments with contact, where it proved to be a very promising and versatile approach to ensure robustness and stability even in the presence of discontinuities and large tracking errors.

In NPC, a passivity observer monitors the power flow in and out of the transfer system. If the transfer system generates more power on the interface to the experimental system than on the interface to the numerical system, it is said to be active and thus unstable. In this case, an artificial damping force is added to the force feedback to the numerical system in order to restore the passivity, hence the stability. In case of a one-dimensional RTHS experiment with the interface degree of freedom (DoF) z_{IP} and interface force F_{IP} (F_m as measured interface force, respectively), the power flow between the subsystems is calculated as follows:

$$P^{NUM} = \dot{z}_{IP} \cdot F_m^{NPC} \tag{5.4}$$

$$P^{EXP} = \dot{z}'_{IP} \cdot F_{IP} \approx \dot{z}'_{IP} \cdot F_m \tag{5.5}$$

Note that in Eq. 5.4, which calculates the power flow between the numerical system and the transfer system, the force F_m^{NPC} also includes the added artificial damping, that is, $F_m^{NPC} = F_m + F_d$. Furthermore, in Eq. 5.5, which calculates the power flow between the experimental and the transfer system, it is assumed that $F_{IP} \approx F_m$, since the actual interface force is not accessible, but only the measured force. As stated above, the transfer system is classified as active if $P^{EXP} > P^{NUM}$, that is, $P_{error} = P^{EXP} - P^{NUM} > 0$. Based on this condition, the damping force is calculated:

$$F_d = \begin{cases} G_d \cdot \frac{\tilde{P}_{error}}{\tilde{P}_{tot}} \cdot \dot{z}_{IP} & \text{if } \tilde{P}_{error} > 0 \\ 0 & \text{if } \tilde{P}_{error} \leq 0 \end{cases} \tag{5.6}$$

Herein, $P_{tot} = P^{EXP} + P^{NUM}$, that is, the total power, is used to normalize the error power P_{error}, for the calculation of the damping gain. Thus, this approach is referred to as *normalized* passivity control. The tuning parameter G_p can be adjusted to adapt the damping magnitude. The artificial damping force F_d is then added to the measured interface force and the total force F_m^{NPC} is used within the numerical system. Note that $\tilde{\bullet}$ indicates a filtering with a first-order lowpass filter with the transfer function $G_{\mathrm{LP}}(s) = (T_{\mathrm{LP}}s + 1)^{-1}$ in order to smooth out the potentially noisy signals.

In order to extend this one-dimensional NPC to our multidimensional system, we implemented an individual NPC for each interface DoF. Hence, the passivity is monitored alongside each interface DoF individually. If one of these DoFs becomes active, damping is only added in this direction and the other DoFs are not affected. In this preliminary implementation, we did not tune each NPC individually, but we use the same parameterization for each of the interface DoF based on our experience from the one-dimensional RTHS experiments. The parameters are also given in Table 5.1. As will be shown in the next section, this resulted in satisfactory behavior of the NPC, but we plan individual tuning and adaption to further improve the performance in future work. The only adaption to the one-dimensional approach described above was an additional lowpass filtering of the damping force using a filter with the transfer function $G(s) = (0.005s + 1)^{-1}$ for the artificial damping force in x- and y-direction and $G(s) = (0.05s + 1)^{-1}$ for the rotational DoF. This was done to further smooth out the damping forces in order to avoid high force peaks in $F_{\mathrm{m}}^{\mathrm{NPC}}$, which is used for the numerical time integration in the numerical subsystem.

5.5 Simulation Results

In order to investigate the behavior of the planar system shown in Fig. 5.2, we performed two virtual RTHS tests. One RTHS simulation with the use of the NPC and one without the use of NPC. Furthermore, we computed the reference solution, which corresponds to the actual behavior of the planar system we want to investigate with RTHS. Consequently, for the reference solution, the transfer system is assumed to have ideal transfer behavior, that is, $\mathbf{q}'_{\mathrm{IP}} = \mathbf{q}_{\mathrm{IP}}$ and $\mathbf{F}_{\mathrm{m}} = \mathbf{F}_{\mathrm{IP}}$. Using this reference,

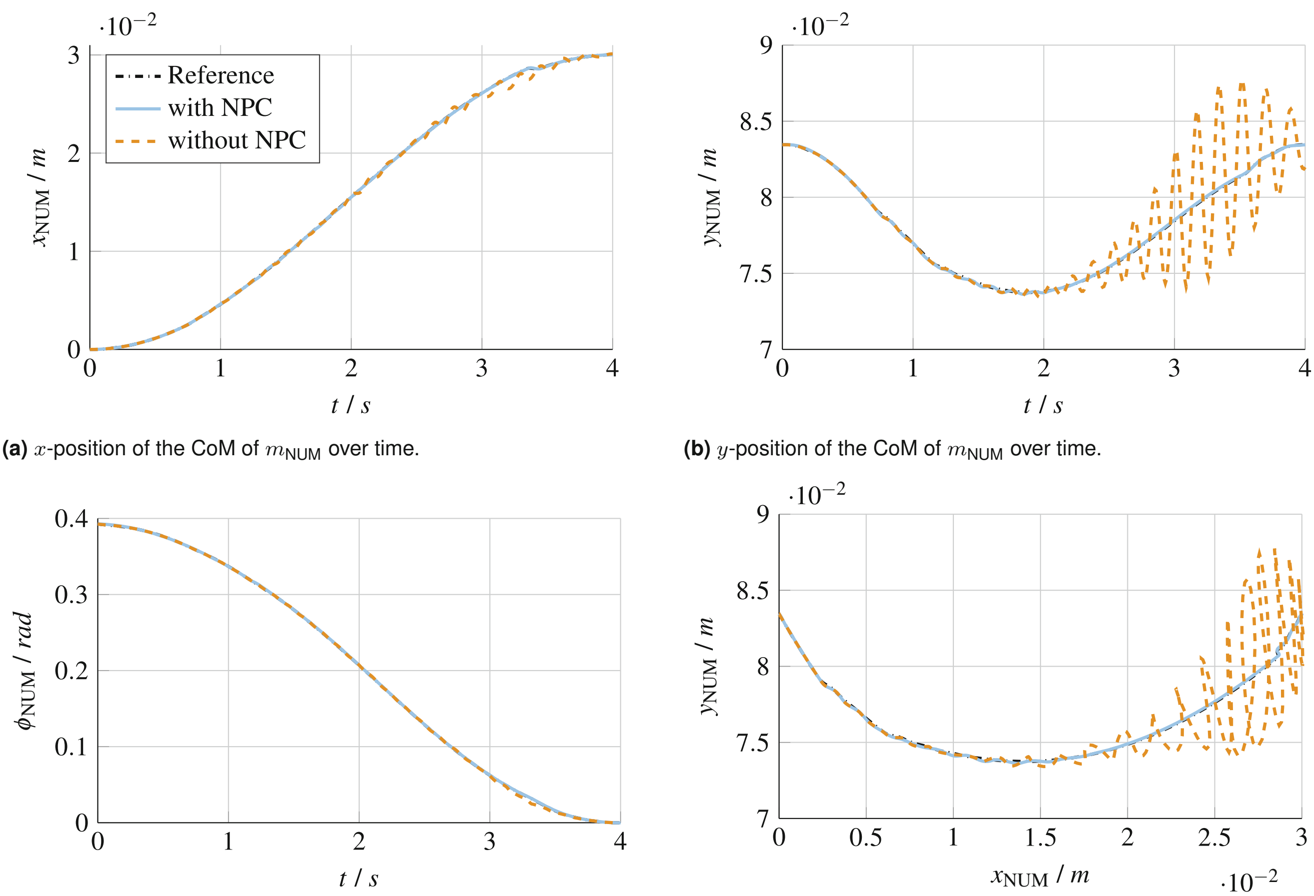

(a) x-position of the CoM of m_{NUM} over time.

(b) y-position of the CoM of m_{NUM} over time.

(c) Rotation of m_{NUM} over time.

(d) y-position of the CoM of m_{NUM} over its x-position.

Fig. 5.3 Motion of the CoM of m_{NUM} with and without the use of NPC. Additionally, the reference trajectories are shown, which correspond to the actual motion of the reference system, respectively the results with an ideal transfer system. Note that the difference between the RTHS trajectories with NPC and the reference trajectories is barely visible in these figures

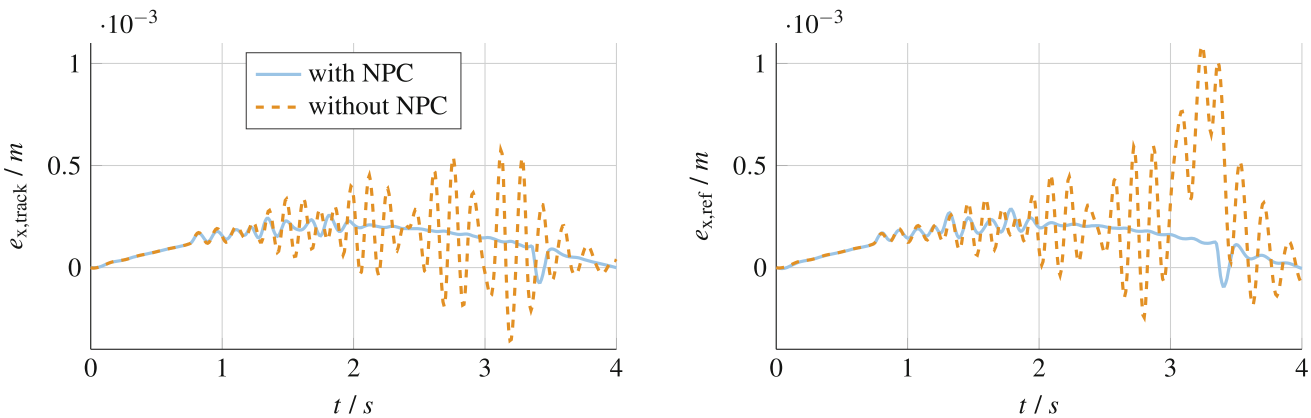

(a) Tracking error in x-direction, that is $e_{\text{x,track}} = x_{\text{IP}} - x'_{\text{IP}}$.

(b) Reference error in x-direction, that is $e_{\text{x,ref}} = x^{\text{Ref}}_{\text{IP}} - x'_{\text{IP}}$.

Fig. 5.4 Tracking and reference error exemplary for the x-direction in the RTHS simulation with and without the use of NPC

we are able to assess the fidelity of the RTHS test outcome. In Fig. 5.3, the motion of the CoM of m_{NUM} is visualized for all three simulations. Furthermore, in the Appendix, the motion of the CoM of m_{EXP} is shown in Fig. 5.5 as well as the interface forces in Fig. 5.6.

From observing these figures, we can confirm that also in the multidimensional case, RTHS experiments with contact are prone to instabilities. Without the use of NPC, the whole system undergoes high-magnitude oscillations, especially in the y-direction. These oscillations are unwanted as they do not represent the real behavior of the reference system. Consequently, this not only heavily deteriorates the test fidelity, but also could damage the test rig, if a real nonvirtual RTHS experiment would be performed. Furthermore, we confirm our observations from the one-dimensional RTHS experiments that also in the multidimensional case the stability of the RTHS tests correlates with the damping in the numerical substructure ($k_{\text{d,x}}$, $k_{\text{d,y}}$ and $k_{\text{d},\phi}$). As we chose rather low values for the damping in the numerical substructure (see Table 5.1), the magnitude of the unwanted oscillation increased. Conversely, for higher damping values in the numerical substructure (e.g., $k_{\text{d,x}} = k_{\text{d,x}} = 200$ Ns/m), no unwanted oscillation was observed and thus a stable RTHS experiment could be performed. The applicability of NPC and its ability to provide stable RTHS experiments is demonstrated in our simulations. In Fig. 5.3 (and Figs. 5.5 and 5.6, respectively), it can be seen how the unwanted oscillation observed without the NPC are damped out by the artificial damping force. Furthermore, it can be observed that each individual passivity controller damps out the unwanted oscillations in the respective directions. The heavy unwanted oscillations in y-directions are sufficiently damped as well as the rather small oscillations in x-directions, without deteriorating each other's damping performance. Additionally, the rotational DoF ϕ_{NUM}, where almost no oscillations are present, is not influenced by the artificial damping in x- and y-directions.

In Fig. 5.4, the tracking and reference errors are shown with and without NPC, exemplary for the x-direction. The tracking-error quantifies the actuator's ability to track its desired trajectories and is thus calculated as $e_{\text{x,track}} = x_{\text{IP}} - x'_{\text{IP}}$. The reference error quantifies the ability of the RTHS test to replicate the true dynamics of the reference system. We define the following error for the motion of the interface point in the reference simulation and the actual motion of the interface point in the RTHS test: $e_{\text{x,ref}} = x^{\text{Ref}}_{\text{IP}} - x'_{\text{IP}}$. In Fig. 5.4, two important observations can be made. Firstly, that the reference error and the tracking error are correlated. Thus, the major cause for the fidelity deterioration is the imperfect actuator tracking. Secondly, it can be seen that the NPC damps out oscillations, but generally does not improve the tracking performance as a major tracking and reference error is still present, also with the use of NPC. Consequently, NPC can be used in order to maintain the stability of the RTHS experiments, but further control approaches (e.g., feedforward control like iterative learning control [12]) have to be considered to improve the tracking performance and thus the test fidelity. This extends our conclusions made in [14] to the multidimensional case.

5.6 Conclusion

In this contribution, we presented our next step toward the testing of foot prostheses using RTHS. Hereby, we aim for the extension and validation of our actuator control methods for stable and robust RTHS experiments with contact that were until now only validated for a one-dimensional RTHS experiment. In order to test our methods using a multidimensional RTHS experiment with contact, we designed a simplified planar foot prosthesis model to be investigated with RTHS. It consists of two simple rigid bodies connected using spring-damper couplings and includes ground contact modeling in horizontal and vertical directions. The simplicity of the system allows us to obtain a reference simulation to assess the fidelity of the RTHS results. For this system, we set up a virtual RTHS experiment. In this digital twin of a real RTHS experiment, also the transfer system and the experimental system are simulated numerically. This gives us the ability to gain a first experience in the application of NPC and in future work further control methods in a multidimensional RTHS experiment. First results of virtual RTHS tests were presented, in which we show that also in the multidimensional case RTHS experiments are prone to instabilities: The system shows unwanted high-magnitude oscillations that not only deteriorate the test fidelity but also could damage the test rig. This is especially true for system configurations with low damping in the numerical substructure. This is in line with our results in previous work investigating a one-dimensional RTHS experiment. In order to counter these instabilities, we implemented NPC. In our multidimensional extension of NPC, we implemented individual passivity observers for each interface DoF and added an artificial damping force in the respective unstable direction. Our simulation results show the applicability of this approach as the unwanted oscillations were damped out and a stable RTHS experiment could be ensured. To conclude, the designed system seems to be promising to further extend our previously developed control methods for RTHS with contact to a multidimensional case. In doing so, we make these methods ready to be applied successfully for the investigation of foot prostheses with RTHS. In future work, we aim for an experimental realization of the system and its RTHS test to validate the results obtained using the virtual RTHS.

5.7 Appendix

See Figs. 5.5 and 5.6.

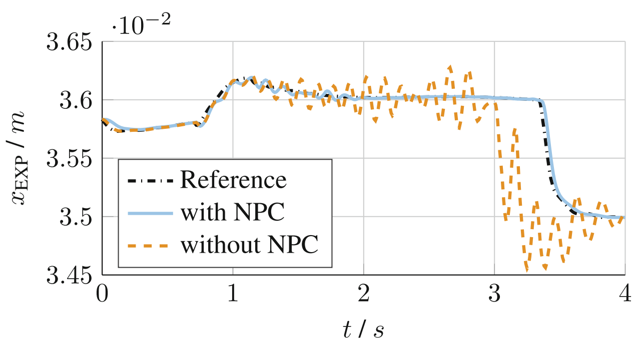

(a) x-position of the CoM of m_{EXP} over time.

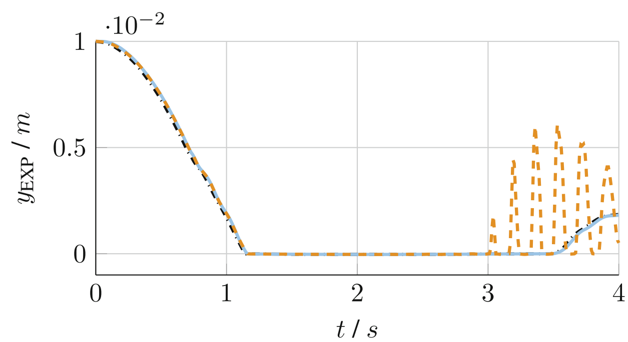

(b) y-position of the CoM of m_{EXP} over time.

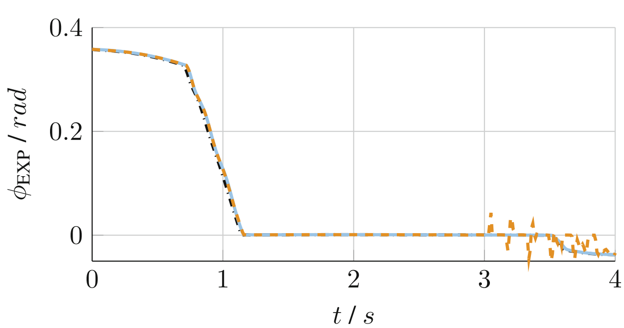

(c) Rotation of m_{EXP} over time.

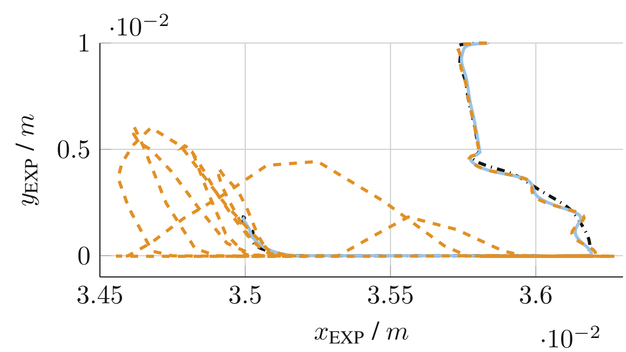

(d) y-position of the CoM of m_{EXP} over its x-position.

Fig. 5.5 Motion of the CoM of m_{EXP} with and without the use of NPC. Additionally, the reference trajectories are shown, which correspond to the actual motion of the reference system, respectively the results with an ideal transfer system

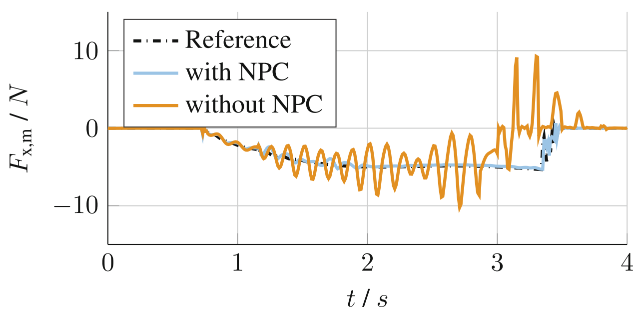

(a) Interface force between m_{NUM} and m_{EXP} in x-direction.

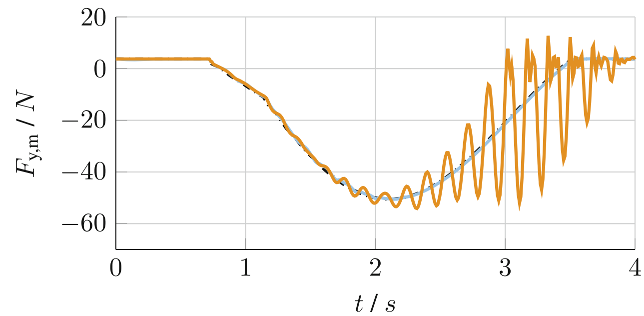

(b) Interface force between m_{NUM} and m_{EXP} in y-direction.

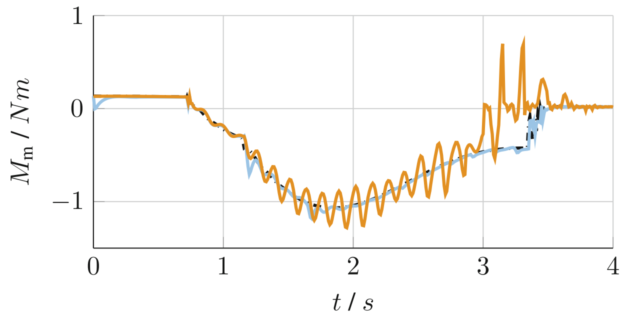

(c) Interface moment between m_{NUM} and m_{EXP}.

Fig. 5.6 Interface forces and moment between the numerical and the experimental substructure. Note that in case of NPC the displayed force is F_m^{NPC}, which includes the artificial damping force added by the NPC

Acknowledgments Part of this work was funded by the Deutsche Forschungsgemeinschaft (DFG, German Research Foundation), Project Number 450801414.

References

1. Walter, N., Alt, V., Rupp, M.: Lower limb amputation rates in Germany. Medicina **58**(1) (2022). https://doi.org/10.3390/medicina58010101
2. Gailey, R., Allen, K., Castles, J., Kucharik, J., Roeder, M.: Review of secondary physical conditions associated with lower-limb amputation and long-term prosthesis use. J. Rehab. Res. Develop. **45**, 15–29 (2008). https://doi.org/10.1682/jrrd.2006.11.0147
3. Murphy, D.: 20 - Gait Deviations after Limb Loss. In: Fundamentals of Amputation Care and Prosthetics. Demos Medical Publishing, New York City (2013)
4. Marinelli, C.: Design, Development and Engineering of a Bench for Testing Lower Limb Prosthesis, With Focus on High-Technological Solutions. PhD thesis. Politecnico di Milano (2016)
5. Insam, C., Ballat, L.-M., Lorenz, F., Rixen, D.J.: Hardware-in-the-loop test of a prosthetic foot. Appl. Sci. **11**(20) (2021). https://doi.org/10.3390/app11209492
6. Blakeborough, A., Williams, M.S., Darby, A.P., Williams, D.M.: The development of real-time substructure testing. R. Soc. **359**(1786), 1869–1891 (2001)
7. Williams, M.S.: Real-time hybrid testing in structural dynamics. In: 5th Australasian Congress on Applied Mechanics, ACAM 2007, vol. 1 (2007)
8. Plummer, A.R.: Model-in-the-loop testing. Proc. Inst. Mech. Eng. Part I J. Syst. Control Eng. **220**(3), 183–199 (2006). https://doi.org/10.1243/09596518JSCE207
9. Yang, Z., Iravani, P., Plummer, A.R., Pan, M.: Investigation of hardware-in-the-loop walking/running test with spring mass system. Towards Auton. Rob. Syst., 126–133 (2017). https://doi.org/10.1007/978-3-319-64107-2
10. Insam, C., Bartl, A., Rixen, D.J.: A step towards testing of foot prostheses using real-time substructuring (RTS). In: Special Topics in Structural Dynamics & Experimental Techniques, vol. 5, pp. 1–9. Springer International Publishing, Berlin (2020)
11. Predovic, J.: Walking Cycle Man. https://svg-clipart.com/man/YS0etCS-walking-cycle-manclipart. Accessed 05 Oct 2022
12. Insam, C., Kist, A., Rixen, D.J.: High fidelity real-time hybrid substructure testing using iterative learning control. In: ISR – 52nd International Symposium on Robotics. VDE Verlag Berlin Offenbach (2020)
13. Insam, C., Peiris, L.D.H., Rixen, D.J.: Normalized passivity control for hardware-in-the-loop with contact. Int. J. Dyn. Control **9**(4), 1471–1477 (2021). https://doi.org/10.1007/s40435-021-00790-8

14. Insam, C., Kist, A., Schwalm, H., Rixen, D.J.: Robust and high fidelity real-time hybrid substructuring. Mech. Syst. Sig. Proces. **157** (2021). https://doi.org/10.1016/j.ymssp.2021.107720
15. Insam, C., Göldeli, M., Klotz, T., Rixen, D.J.: Comparison of feedforward control schemes for real-time hybrid substructuring (RTHS). In: Dynamic Substructures, vol. 4, pp. 1–14. Springer International Publishing, New York City (2021)
16. Geyer, H., Herr, H.: A muscle-reflex model that encodes principles of legged mechanics produces human walking dynamics and muscle activities. IEEE Trans. Neural Syst. Rehab. Eng. **18**(3), 263–273 (2010). https://doi.org/10.1109/TNSRE.2010.2047592
17. Peiris, L.D.H., Plummer, A., du Bois, J.: Normalised passivity control for robust tuning in real-time hybrid tests. Int. J. Robust Nonlin. Control **32**(7), 4355–4375 (2022)